Acta Cryst. (1976). B**32**, 998

The Crystal and Molecular Structure of 1,3-Diazanaphthalene

BY C. HUISZOON

Chemical Physics Laboratory, Twente University of Technology, P.O. Box 217, *Enschede, The Netherlands*

(*Received* 2 *June* 1975; *accepted* 27 *August* 1975)

X-ray diffraction data of 1,3-diazanaphthalene or quinazoline have been collected at room temperature, using a computer-controlled Philips diffractometer (PW 1100). The unit cell is triclinic, $P\bar{1}$ (assumed), two molecules in the asymmetric unit, with $a=11{\cdot}983$ (1), $b=7{\cdot}8555$ (5), $c=7{\cdot}4660$ (5) Å, $\alpha=91{\cdot}13$ (1), $\beta=99{\cdot}84$ (1), $\gamma=108{\cdot}73$ (1)°, $Z=4$. The structure was solved by direct methods and refined in two blocks by the full-matrix least-squares method to an R index of 0·046 (weighted R 0·042). Within experimental error, both molecules in the asymmetric unit can be considered identical in shape, with small (~0·01 Å), but significant, deviations from planarity. The crystals invariably showed twinning. The orientations of the components of the twin differ by a rotation of 180° around the [211] direct axis.

Introduction

In our laboratory the chemical and physical properties of diazanaphthalenes are studied. In earlier papers the crystal and molecular structures of 2,3-diazanaphthalene (phthalazine) (Huiszoon, van de Waal, van Egmond & Harkema, 1972); anhydrous 1,8-diazanaphthalene (Clearfield, Sims & Singh, 1972); the dihydrates of 1,5-diazanaphthalene (orthorhombic form) and 2,6-diazanaphthalene [Brufani, Duranti, Giacomello & Zambonelli (1961) and Brufani, Fedeli, Giacomello, Riccieri & Vaciago (1966) respectively] have been described. In the present paper the crystal and molecular structure of 1,3-diazanaphthalene or quinazoline is described.

Experimental

Small crystals were grown by slow sublimation in vacuum (0·5 Torr) at about 15°C, from commercially available quinazoline (Fluka A.G., Switzerland). Crystals obtained in this way invariably showed twinning, and a twinned specimen was used in the analysis.

A crystal of maximum linear dimensions about 0·4 mm, was mounted in a Lindemann glass capillary. Cell constants and intensity data were obtained with a computer-controlled single-crystal diffractometer (Philips, PW 1100) using crystal-monochromated Mo $K\alpha$ radiation, $\lambda=0{\cdot}7107$ Å. Crystal data are shown in Table 1.

Table 1. *Crystal data for quinazoline at* 20°C

Crystal system: triclinic
Space group: $P\bar{1}$ (assumed, no systematic absences)
$a=11{\cdot}983$ (1), $b=7{\cdot}8555$ (5), $c=7{\cdot}4660$ (5) Å
$\alpha=91{\cdot}13$ (1), $\beta=99{\cdot}84$ (1), $\gamma=108{\cdot}73$ (1)°
$V=653{\cdot}7$ Å^3
$D_m=1{\cdot}30$ g cm^{-3}
$D_c=1{\cdot}322$ g cm^{-3}
$Z=4$
μ(Mo $K\alpha$) $=0{\cdot}89$ cm^{-1}

The twin-law was derived from the orientational matrices obtained for each of the two components of the twinned crystal. Comparison of these matrices showed that the orientations of the direct systems of axes of the two components of the twin differ by a 180° rotation around their [211] direct axes. As a consequence, planes parallel to this axis, *i.e.* planes with indices $2h+k+l=0$, coincide exactly with planes $\bar{h}\bar{k}\bar{l}$ belonging to the other component of the twinned crystal, and the intensities of both reflexions are measured simultaneously. The measured intensities from these reflexions have been corrected for this effect as well as those from planes which coincide only approximately with a reflecting plane of the other component of the twin. In the discussion which follows, the components of the twinned lattice will be called I and II, where component I has the larger volume. To carry out the corrections, the reflexions of component I have been divided into three categories: (i) well separated from reflexions of component II, (ii) close to a reflexion of component II, (iii) at intermediate separation from a reflexion of component II.

In order to classify the reflexions into the three categories (i), (ii) and (iii), the halfwidths, to the 10% intensity level, have been estimated as 0·7° in the χ direction and 0·35° in the θ direction. The intensities have been measured using a $\theta/2\theta$ scan, scan width 1·9°. The horizontal and vertical detector apertures were 2° and 1·5° respectively. From these data the following criteria have been derived: when H is a reflexion of component I of the twin, and K is the reflexion of the other component closest to H, then H belongs to category (i), when $|\chi_H-\chi_K|>1{\cdot}45°$ or $|\varphi_H+\theta_H-\varphi_K-\theta_K|>1{\cdot}2°$; and reflexion H belongs to category (ii) when $|\chi_H-\chi_K|<1{\cdot}45°$ and $|\varphi_H+\theta_H-\varphi_K-\theta_K|<1{\cdot}2°$. Reflexions H not belonging to either (i) or (ii), belong to category (iii). A description of the diffractometer, including the precise meaning of the symbols χ, φ and θ mentioned above, has been given by Hornstra & Vossers (1973).

Intensities of reflexions falling into category (ii) have been corrected using the equation

$$I^c_H=(I^m_H-I^m_K/F)F^2/(F^2-1)\,,$$

where I_H^m is the measured intensity at the position of reflexion H being close to the position of reflexion K of the other component of the twin, F is the volume ratio of the two components, I_H^m and I_K^m are the respective intensities measured at the positions of reflexions H and K of component I and I_H^c is the corrected intensity of reflexion H. Reflexions belonging to category (iii) generally have been removed from the data set, except in those cases where the accompanying reflexion K was insignificant. The volume ratio F of the two components has been determined using reflexions belonging to category (i). Because of the rather large value of F (6·7), the corrections are not of crucial importance.

The scan speed was 0·3° s^{-1} and minimum count 3000. The stationary background was counted during half the measuring time on both sides of the peak. θ values ranged from 3 to 25°.

2298 reflexions were measured, 272 have been removed owing to twinning of the crystal, and 99 have corrected intensities.

Structure determination and refinement

The structure has been solved using the multisolution program *MULTAN* of Germain, Main & Woolfson (1971). The four possible solutions generated by the program were pair-wise identical, one pair representing a trivial solution, the other pair the correct solution.

The statistical averages and distributions of the derived normalized structure factors, the E values, are given in Table 2. In addition the Howell, Phillips &

Table 2. *Statistical averages and distributions of normalized structure factors*

	Data set	Theoretical Centric	Theoretical Non-centric
$\langle\lvert E\rvert\rangle$	0·76	0·798	0·886
$\langle\lvert E\rvert^2-1\rangle$	1·14	0·968	0·736
$\langle\lvert E\rvert\rangle^2$	1·05	1·000	1·000
$\lvert E\rvert>1$	27·0 %	32 %	36·8 %
$\lvert E\rvert>2$	6·4	5·0	1·8
$\lvert E\rvert>3$	0·8	0·3	0·01

Table 3. *Observed and calculated structure factors*

Columns are: h, k, l, $|F_o|$, $|F_c|$. Reflexions marked with * have a corrected value for $|F_o|$ due to twinning.

Rogers (1950) test on centricity and the centre of symmetry test by second harmonic generation, which was negative, were performed. From the results in Table 2, and the results of the tests, the centrosymmetric space group $P\bar{1}$ has been assumed to be the correct space group for quinazoline.

The refinement was carried out by the program *ORFLS* of Busing, Martin & Levy (1962) in two blocks each of 116 parameters dealing with positional and thermal parameters of one molecule, a scale factor and an extinction factor (Larson, 1969). Atomic scattering factors for C and N were calculated from atomic wavefunctions given by Clementi (1965). The scattering factor for H was taken from Stewart, Davidson & Simpson (1965). The function minimized and the weighting scheme were identical to those described in the paper on phthalazine (Huiszoon *et al.*, 1972). Absolute values of the observed and calculated significant structure factors have been listed in Table 3. The *R* index obtained was 0·046 (weighted *R* 0·042). The number of significant reflexions used for the refinement was 1599.

Structural results

There are two crystallographically independent molecules in the unit cell. The atoms which are numbered from 1 to 16 form molecule *A*, the atoms numbered 17 to 32 form molecule *B*. The final atomic positional and thermal parameters are given in Table 4.

Bond lengths and bond angles occurring in the molecules *A* and *B* are given in Fig. 1. Comparing the geometries of the molecules *A* and *B*, it is seen from Fig. 1 that all corresponding bond lengths between the heavy atoms are equal to each other within the standard deviation. Of the bond lengths in which H atoms are involved, three corresponding lengths equal each other within the standard deviation and three are equal within twice the standard deviation. Only one bond angle, C(9)–C(8)–H(6) in molecule *A*, differs slightly more than one standard deviation from the corresponding bond angle, C(25)–C(24)–H(32), of molecule *B*. The equations of the best planes through the heavy atoms of each of the molecules, and the atomic deviations

Table 4. *Atomic parameters for* 1,3-*diazanaphthalene*

The anisotropic temperature factor is of the form $\exp\left[-2\pi^2(h^2a^{*2}u_{11}+\ldots 2hka^*b^*U_{12}+\ldots)\right]$ and the isotropic temperature factor $\exp(-8\pi^2U\sin^2\theta/\lambda^2)$. The positional parameters are $\times 10^4$ (for the H atoms $\times 10^3$). The thermal parameters for non-hydrogen atoms are given in 10^{-3} Å^2, the values of U are in Å^2. Standard deviations are shown in parentheses and refer to the last digits.

	x	y	z	U_{11}	U_{22}	U_{33}	U_{12}	U_{13}	U_{23}
Molecule *A*									
N(1)	−914 (1)	2546 (2)	3103 (2)	40 (1)	51 (1)	61 (1)	12 (1)	6 (1)	3 (1)
C(2)	−311 (2)	3547 (3)	1983 (3)	54 (1)	56 (1)	49 (1)	16 (1)	2 (1)	4 (1)
N(3)	886 (1)	4422 (2)	2222 (2)	52 (1)	57 (1)	49 (1)	9 (1)	8 (1)	5 (1)
C(4)	1504 (2)	4265 (2)	3794 (3)	40 (1)	45 (1)	54 (1)	5 (1)	11 (1)	0 (1)
C(5)	1651 (2)	3091 (2)	6865 (3)	56 (1)	47 (1)	55 (1)	17 (1)	2 (1)	3 (1)
C(6)	1073 (2)	2071 (3)	8084 (3)	85 (2)	59 (1)	54 (1)	30 (1)	7 (1)	11 (1)
C(7)	−167 (2)	1178 (3)	7656 (4)	85 (2)	54 (1)	69 (2)	26 (1)	36 (1)	20 (1)
C(8)	−825 (2)	1314 (3)	6036 (3)	51 (1)	49 (1)	70 (1)	16 (1)	24 (1)	9 (1)
C(9)	−254 (1)	2373 (2)	4739 (3)	40 (1)	35 (1)	52 (1)	15 (1)	14 (1)	1 (1)
C(10)	988 (1)	3252 (2)	5155 (3)	43 (1)	32 (1)	47 (1)	13 (1)	8 (1)	−1 (1)
H(11)	−78 (2)	366 (2)	82 (3)	0·061 (6)					
H(12)	239 (2)	488 (2)	402 (2)	0·060 (6)					
H(13)	257 (2)	373 (3)	708 (3)	0·070 (6)					
H(14)	151 (2)	196 (3)	927 (3)	0·072 (6)					
H(15)	−59 (2)	47 (3)	855 (3)	0·083 (7)					
H(16)	−169 (2)	70 (3)	567 (3)	0·063 (6)					
Molecule *B*									
N(17)	3607 (1)	1140 (2)	2794 (2)	43 (1)	61 (1)	68 (1)	13 (1)	16 (1)	3 (1)
C(18)	4379 (2)	2723 (3)	3430 (3)	57 (1)	52 (1)	72 (1)	20 (1)	18 (1)	1 (1)
N(19)	5588 (1)	3273 (2)	3663 (2)	49 (1)	45 (1)	71 (1)	11 (1)	11 (1)	−1 (1)
C(20)	6039 (2)	2045 (2)	3218 (3)	38 (1)	49 (1)	56 (1)	8 (1)	4 (1)	3 (1)
C(21)	5815 (2)	−1066 (3)	2095 (3)	56 (1)	53 (1)	54 (1)	22 (1)	3 (1)	5 (1)
C(22)	5058 (2)	−2746 (3)	1463 (3)	85 (1)	49 (1)	60 (1)	26(1)	11 (1)	5 (1)
C(23)	3818 (2)	−3148 (3)	1245 (3)	83 (1)	45 (1)	53 (1)	1 (1)	11 (1)	2 (1)
C(24)	3333 (2)	−1889 (3)	1671 (3)	53 (1)	56 (1)	53 (1)	−4 (1)	10 (1)	1 (1)
C(25)	4092 (2)	−137 (2)	2348 (2)	45 (1)	46 (1)	40 (1)	7 (1)	12 (1)	7 (1)
C(26)	5333 (1)	269 (2)	2557 (2)	41 (1)	44 (1)	38 (1)	11 (1)	6 (1)	9 (1)
H(27)	403 (1)	365 (3)	385 (3)	0·067 (6)					
H(28)	693 (1)	241 (2)	339 (2)	0·046 (6)					
H(29)	669 (2)	−73 (2)	232 (3)	0·059 (6)					
H(30)	540 (2)	−367 (3)	113 (3)	0·084 (6)					
H(31)	327 (2)	−443 (3)	77 (3)	0·090 (7)					
H(32)	247 (2)	−217 (3)	156 (3)	0·066 (6)					

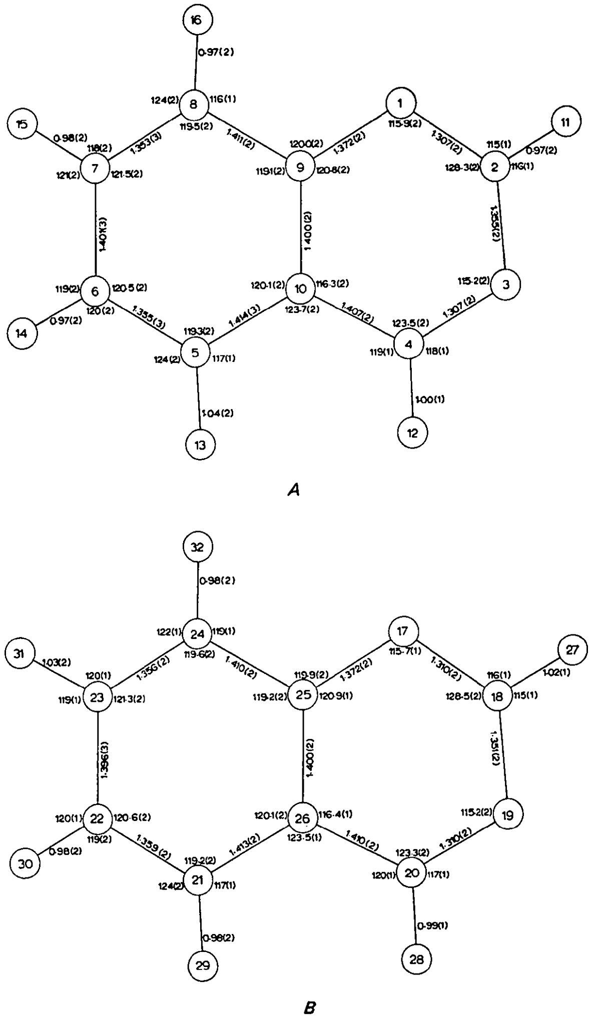

Fig. 1. Bond lengths and bond angles of the two crystallographically independent molecules, *A* and *B*, of quinazoline. Distances are in Å, angles in degrees. Standard deviations of the last digits are shown in parentheses. Note the rather low values of the CNC bond angles.

from these planes are listed in Table 5. It is seen that the molecules show a deviation from planarity which is small but significant, and is expected to be a molecular property rather than an effect caused by the packing as the following qualitative argument shows.

From Fig. 2, drawn with the aid of the program *STER* written by van de Waal (1973), it is seen that the structure consists of columns of parallel molecules along either the *b* or *c* crystallographic axis. The interplanar spacings within the columns do not differ very much. In the column along the *b* axis, between molecule *A* at x,y,z, and the molecules at $-x,-y,1-z$,

Table 5. *Atomic deviations from best planes through the heavy atoms*

Equations of best planes are given as $n_xx+n_yy+n_zz=d$, where n_x, n_y, and n_z are the direction cosines of the normal to the plane with respect to an orthogonal system of axes according to Williams (1969). d is the distance of the plane to the origin (Å). The components of the normals to the planes, with respect to the triclinic cell system of axes, are also given. The numbering of the atoms is in accordance with Fig. 1. A plus sign means a deviation towards the reader, a minus sign represents a deviation away from the reader.

Molecule *A*

Equation of plane $-0{\cdot}2218x+0{\cdot}8934y+0{\cdot}3906z=3{\cdot}2633$ Å
Components of normal in fractional coordinates $-0{\cdot}01299$, $0{\cdot}1084$, $0{\cdot}05327$

N(1)	+0·012 (1) Å	C(6)	+0·010 (2) Å
C(2)	+0·014 (2)	C(7)	−0·007 (2)
N(3)	−0·011 (1)	C(8)	−0·013 (2)
C(4)	−0·011 (2)	C(9)	−0·005 (1)
C(5)	+0·011 (2)	C(10)	−0·001 (1)

Molecule *B*

Equation of plane $-0{\cdot}1394x-0{\cdot}3287y+0{\cdot}9341z=1{\cdot}5751$ Å
Components of normal in fractional coordinates $0{\cdot}003398$, $-0{\cdot}03779$, $0{\cdot}1274$

N(17)	−0·002 (1) Å	C(22)	+0·011 (2) Å
C(18)	+0·015 (2)	C(23)	−0·001 (2)
N(19)	+0·000 (1)	C(24)	−0·008 (2)
C(20)	−0·012 (2)	C(25)	−0·004 (1)
C(21)	+0·001 (2)	C(26)	−0·001 (1)

Angle between the planes of two crystallographically independent molecules is 84·1°.

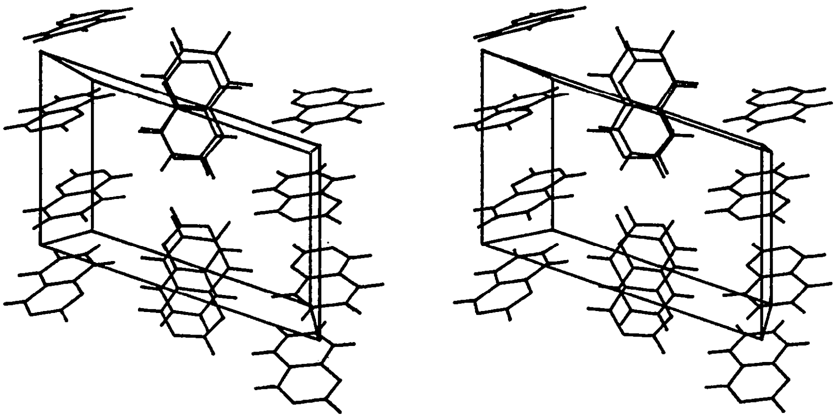

Fig. 2. Stereoscopic pair showing the molecular packing of quinazoline. The *a* axis points to the right, the vertical axis is the *b* axis, the *c* axis points towards the reader.

and $-x,1-y,1-z$, they are 3·48 and 3·53 Å respectively. In the other column the interplanar spacings between molecule *B*, at x,y,z, and its parallel neighbours at $1-x,-y,1-z$ and $1-x,-y,-z$ are 3·62 and 3·46 Å respectively. The intermolecular contacts, within 0·1 Å greater than the relevant van der Waals radii (Kitaigorodsky, 1961), are listed in Table 6. In addition, Fig. 3 gives the projections of the neighbouring parallel molecules on the planes of the molecules *A* and *B*. From Table 6 and Fig. 3 it is seen that the molecules *A* and *B* are in different surroundings. This result and the similarity in non-planarity between the two molecules, suggests that the non-planarity does not originate from packing effects, but is a molecular property. This statement is made uncertain because the similarity in non-planarity does not hold for all ten heavy atoms of each molecule: the deviations of the N atoms and the C atoms at the fifth positions differ between molecules.

Table 6. *Intermolecular contacts* (Å) *within* 0·1 Å *greater than the sum of the relevant van der Waals radii* (*Kitaigorodsky*, 1961)

The reference molecules are at x,y,z, the translated molecules are listed second. The second atoms are accompanied by the symbol *I*/*uvw* indicating the operation applied to the second atoms: $I=1$ represents the identity operation, $I=2$ the operation to $-x,-y,-z$. *u*, *v* and *w* are the fractional translations along the cell axes.

Molecule *A* to its parallel neighbours			
	C(7)–C(9)	2/001	3·50
	C(8)–C(9)	2/001	3·60
	C(8)–C(10)	2/001	3·61
	C(2)–C(10)	2/011	3·64
	C(2)–C(5)	2/011	3·66
	C(4)–C(9)	2/011	3·66
Molecule *B* to its parallel neighbours			
	C(18)–C(21)	2/101	3·63
	C(20)–C(25)	2/101	3·67
	C(20)–C(22)	2/100	3·64
	C(20)–C(23)	2/100	3·48
	C(21)–C(25)	2/100	3·48
	C(21)–C(26)	2/100	3·65
	C(22)–C(26)	2/100	3·65
Molecule *A* other contacts			
	N(1)—H(28)	1/$\bar{1}$00	2·60
	N(3)—H(11)	2/010	2·76
	C(4)—C(24)	1/010	3·68
	H(11)–H(32)	2/000	2·40
	H(11)–N(3)	2/010	2·76
	H(12)–N(19)	2/111	2·68
	H(12)–C(20)	2/111	3·03
	H(12)–C(23)	1/010	3·04
	H(13)–N(19)	2/111	2·80
	H(16)–N(17)	2/001	2·74
Molecule *B* other contacts			
	N(17)–H(16)	2/001	2·74
	N(19)–H(12)	2/111	2·68
	N(19)–H(13)	2/111	2·80
	C(20)–H(12)	2/111	3·03
	C(24)–C(4)	1/0$\bar{1}$0	3·68
	H(28)–N(1)	1/100	2·60
	H(32)–H(11)	2/000	2·40

Fig. 4 shows an *ORTEP* drawing (Johnson, 1965) of both molecules. The close resemblance of the thermal motion of the individual atoms of both molecules is clearly demonstrated.

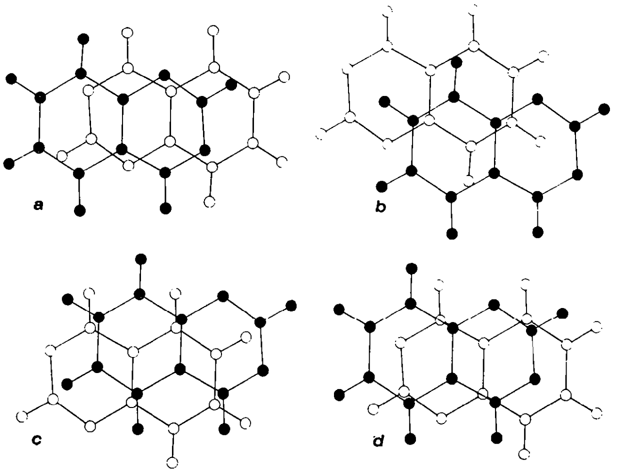

Fig. 3. Projections of the neighbouring parallel molecules on the planes of the molecules *A* and *B*. The atoms of molecules *A* and *B* are indicated by black dots; (*a*) molecule *A* and the molecule at $-x,1-y,1-z$; (*b*) molecule *A* and the molecule at $-x,-y,1-z$; (*c*) molecule *B* and the molecule at $1-x,-y,-z$; (*d*) molecule *B* and the molecule at $1-x,-y,1-z$.

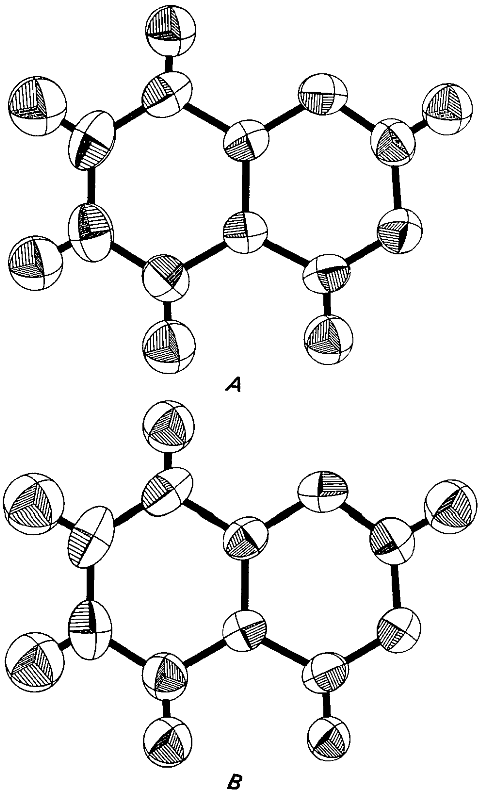

Fig. 4. Thermal ellipsoids drawn at the 50% probability level of molecule *A* and *B*.

The author thanks Mr H. A. Plessius and Dr S. Harkema for their help during the early stages of the investigation. Mr P. A. Kroon of the Rijksuniversiteit Groningen is thanked for performing part of the refinement and Dr J. P. Dougherty of North American Philips, for carrying out the test with the second harmonic analyser.

References

Brufani, M., Duranti, D., Giacomello, G. & Zambonelli, L. (1961). *Gazz. Chim. Ital.* **91**, 287–298.

Brufani, M., Fedeli, W., Giacomello, G., Riccieri, F. M. & Vaciago, A. (1966). *Atti Acad. Nazl. Lincei Rend. Classe Sci. Fis. Mat. Nat.* **40**, 187–193.

Busing, W. R., Martin, K. O. & Levy, H. A. (1962). *ORFLS*. Oak Ridge National Laboratory Report ORNL-TM-305.

Clearfield, A., Sims, M. J. & Singh, P. (1972). *Acta Cryst.* B**28**, 350–355.

Clementi, E. (1965). *IBM Res. Dev.* **9**, 2–19.

Germain, G., Main, P. & Woolfson, M. M. (1971). *Acta Cryst.* A**27**, 368–376.

Hornstra, J. & Vossers, H. (1973). *Philips Tech. Rev.* **33**, 61–73.

Howells, E. R., Phillips, D. C. & Rogers, D. (1950). *Acta Cryst.* **3**, 210–214.

Huiszoon, C., van de Waal, B. W., van Egmond, A. B. & Harkema, S. (1972). *Acta Cryst.* B**28**, 3415–3419.

Johnson, C. K. (1965). *ORTEP*. Oak Ridge National Laboratory Report ORNL-3794.

Kitaigorodsky, A. I. (1961). *Organic Chemical Crystallography*. New York: Consultants Bureau.

Larson, A. C. (1969). *Crystallographic Computing*, edited by F. R. Ahmed, pp. 291–294. Copenhagen: Munksgaard.

Stewart, R. F., Davidson, E. R. & Simpson, W. T. (1965). *J. Chem. Phys.* **42**, 3175–3187.

Waal, B. W. van de (1973). *STER, a Fortran Program for Drawing Crystal Structures*. Progress Report 12, Chemical Physics Laboratory, Twente Univ. of Technol., Enschede, The Netherlands.

Williams, D. E. (1969). *Acta Cryst.* A**25**, 464–470.

Acta Cryst. (1976). B**32**, 1003

A Powder Neutron Diffraction Investigation of the Oxygen Vacancy Distribution in $4H$ $\mathrm{Ba_{0\cdot5}Sr_{0\cdot5}MnO_{2\cdot84}}$ and the Magnetic Structure of $4H$ $\mathrm{Ba_{0\cdot1}Sr_{0\cdot9}MnO_{2\cdot96}}$

By A. J. Jacobson and A. J. W. Horrox

Inorganic Chemistry Laboratory, South Parks Road, Oxford, OX1 3QR, England

(*Received* 21 *June* 1975; *accepted* 18 *July* 1975)

The structure and O vacancy distribution in $4H$ $\mathrm{Ba_{0\cdot5}Sr_{0\cdot5}MnO_{2\cdot84}}$ and the magnetic structure of $4H$ $\mathrm{Ba_{0\cdot1}Sr_{0\cdot9}MnO_{2\cdot96}}$ have been determined by profile analysis of powder neutron diffraction data. In $\mathrm{Ba_{0\cdot5}Sr_{0\cdot5}MnO_{2\cdot84}}$ the O vacancies are found in hexagonal $\mathrm{(Ba,Sr)O_3}$ layers which suggests that the $\mathrm{Mn^{3+}}$ ions are coordinated by O in edge-sharing trigonal bipyramids. The antiferromagnetic structure of $\mathrm{Ba_{0\cdot1}Sr_{0\cdot9}MnO_{2\cdot96}}$ has alternate Mn atoms along **c** with opposite spin and the spin direction in the basal plane. The sublattice magnetization was found to be $gS = 2\cdot42\ (4)$ at $4\cdot2K$.

Introduction

Perovskite related $\mathrm{ABO_3}$ mixed metal oxides have structures which are ideally based on close-packing of $\mathrm{AO_3}$ layers with B cations in octahedral sites and which differ in the ratio of the number of cubic to hexagonal layers. Relationships between such structures have been discussed by Katz & Ward (1964).

The $\mathrm{BaMnO_{3-x}}$ and $\mathrm{SrMnO_{3-x}}$ systems are of particular interest in that they exhibit a wide variety of structure types and extensive ranges of non-stoichiometry. Negas & Roth (1970, 1971) have investigated in detail the phase relationships and O composition for both compounds and their main experimental conclusions are summarized in Table 1. In both the amount of cubic stacking increases and the O content decreases with increasing temperature.

Table 1. $\mathrm{BaMnO_{3-x}}$ *in air* (*after Negas & Roth*, 1971) *and* $\mathrm{SrMnO_{3-x}}$ *in air* (*after Negas & Roth*, 1970)

$\mathrm{BaMnO_{3-x}}$ Layer sequence	Temperature (°C)	Oxygen content	% cubic stacking
$2H$	1150	$x=0$	0
$15H$	1150–1300	$0<x<0\cdot02$	20
$8H$	1300–1350	$0\cdot03<x<0\cdot05$	25
$6H$	1350–1475	$0\cdot10<x<0\cdot15$	$33\frac{1}{3}$
$10H$	1475–1550	$0\cdot175<x<0\cdot20$	40
$4H$	1550	$x\sim0\cdot25$	50
$\mathrm{SrMnO_{3-x}}$			
$4H$	1035	$x=0$	50
$4H$	1035–1400	$0<x<0\cdot11$	50
$3C$	1400–1740	$0\cdot26<x<0\cdot38$	100

Negas (1973) also studied the solid solutions $\mathrm{Ba_{1-y}Sr_yMnO_{3-x}}$ and showed that the $2H$, $15H$ and